

Probing spin-orbital-lattice correlations in $4d^4$ systems

Mario Cuoco, Filomena Forte, and Canio Noce

Laboratorio Regionale SuperMat, INFN-CNR, Baronissi (SA), Italy

and Dipartimento di Fisica "E. R. Caianiello," Università di Salerno, I-84081 Baronissi, Salerno, Italy

(Received 21 November 2005; revised manuscript received 10 February 2006; published 22 March 2006)

By means of an exact diagonalization technique, we analyze the ground state configurations that emerge out of the competition between the octahedral distortions, the Coulomb interactions, and the spin-orbit coupling in the case of two effective t_{2g} sites in $4d^4$ configuration. We show that the crystalline field is a suitable quantum control of the magnetic and orbital correlations, leading to predominant antiferromagnetic (ferromagnetic) exchange with ferro- (antiferro-) like orbital correlations in the flat (elongated) octahedral configuration. Moreover, the role of the spin-orbit coupling is investigated with respect to the character of the octahedral deformations. One of the main findings is the occurrence of anisotropic spin patterns with partially filled orbital occupation and coexisting ferro- and antiferrolike correlations in the spin/orbital channel. Finally, the possibility of competing states with partial orbital occupation is amplified when a spin polarizing field is added to the system. Its role in controlling magnetic/orbital correlations is also presented.

DOI: [10.1103/PhysRevB.73.094428](https://doi.org/10.1103/PhysRevB.73.094428)

PACS number(s): 75.50.Ee, 71.10.-w, 75.10.-b

I. INTRODUCTION

Recently, the coupling of spin, orbital, and lattice degrees of freedom in the t_{2g} manifold emerged as a relevant aspect in determining the physical properties of many transition metal oxides¹ such as for instance titanates, vanadates,^{2,3} and ruthenates.⁴ Referring to the class of ruthenates, the Ruddlesden-Popper series $(\text{Sr,Ca})_{n+1}\text{Ru}_n\text{O}_{3n+1}$, where n indicates the number of Ru-O layers for unit cell, has shown, in this respect, complex and intriguing phenomena.

The insulating single layered Ca_2RuO_4 is a representative case of the variety of possible spin and orbital patterns in triple degenerate $4d^4$ systems. One of the puzzling aspects exhibited by this compound refers to the nature of charge/orbital pattern in the t_{2g} subspace. The observation of G-type antiferromagnetism⁵ has been interpreted as a preferential occupation of the d_{xy} orbital (completely filled) with half-filled d_{xz}, d_{yz} sector, in a state with ferro-orbital (FO) type order. On the other hand, x-ray spectroscopy indicated the possibility of having 0.5 holes in the d_{xy} orbital leading to partial occupation of the t_{2g} orbitals, which is attributed to the stabilization of complex orbitals due to the strong spin-orbit coupling.⁶ The discussion has been recently extended and puzzled by the observation, via resonant x-ray diffraction, of an orbital ordering transition at a wave vector characteristic of the antiferromagnetic ordering.⁷ The data show the presence of an orbital order with the same wave vector of the antiferromagnetic one that sets in at lower temperatures, although the contribution of a ferro-orbital component⁸⁻¹⁰ in the ordering pattern cannot be completely excluded.

The application of an external magnetic field¹¹⁻¹⁶ adds extra puzzles and raises several questions about the spin/orbital/lattice dynamics. Indeed, the bilayered $\text{Ca}_3\text{Ru}_2\text{O}_7$ features a Mott-type transition, a metamagnetic transition, and also exhibits colossal magnetoresistance (CMR) phenomena¹³ when a magnetic field is set in. Possible interpretations of the CMR point into the direction of a collapse of an orbitally ordered configuration realized also by demol-

ishing the spin-polarized state. This effect clearly indicates that the orbital and spin degrees of freedom are intimately coupled so that polarizing spins stabilize the orbitally ordered state that prevents electron motion. Conversely, the demolition of the polarized state leads to a melting of the orbitally ordered which in turn produces a drastic drop of the magnetoresistance.^{14,16}

Furthermore, the opportunity of tuning structural modifications induced by both chemical substitution $(\text{Sr,Ca})\text{RuO}_4$,^{17,18} or when an external pressure^{19,20} is applied, has given extra interest toward this class of oxides, stimulating again the investigation of their spin, orbital, and lattice dynamics. With the Sr substitution for Ca, the system $\text{Ca}_{2-x}\text{Sr}_x\text{RuO}_4$ is successively driven from an antiferromagnetic insulator ($x < 0.2$) to an antiferromagnetic correlated metal ($0.2 < x < 0.5$), a nearly ferromagnetic metal for $x \sim 0.5$, a nonmagnetic two-dimensional Fermi liquid for $x \sim 2$, the end member of series, Sr_2RuO_4 , exhibiting an unconventional superconductivity below 1.5 K.²¹ Since the substitution of Sr for Ca is isovalent, the dominant effects are the structural modifications due to the reduced ionic size of Ca compared with Sr, and these distortions correlate with the changes in the magnetic and the electronic properties of the whole system. Three types of structural distortions are identified from experiments:²² RuO_6 octahedron rotation about the c axis; RuO_6 tilting around an axis parallel to the edge of octahedron basal plane; and finally, the flattening or elongation of the RuO_6 along the c axis. In particular, the RuO_6 rotation can enhance the ferromagnetic instability significantly, while the combination of tilting and rotation of RuO_6 is responsible for the enhancement of antiferromagnetic instability. Still, the flattening (elongation) of RuO_6 is a key factor to stabilize an antiferromagnetic (mostly ferromagnetic) ground state.

As a summary of these experimental results, we can state that these systems provide a great opportunity of studying unconventional phenomena dominated by strong correlation effects, especially because the interplay between lattice, spin,

charge, and orbital degrees of freedom can be experimentally controlled by varying some specific external control parameters.

On the theoretical side, the analysis starts considering that, in ruthenates with Ru^{4+} ions, the Hund's rule energy, maximizing the total spin at each Ru site, is not large enough to overcome the e_g - t_{2g} crystal field splitting, leaving empty the e_g manifold. The constraint to accommodate four electrons in the t_{2g} sector imposes a double occupation in one of the three orbitals. Furthermore, the t_{2g} orbitals are expected to have different energies because the RuO_6 octahedra are deformed and the electrons may couple to lattice dynamics via the Jahn-Teller interaction. To explore the phenomenology of these materials, the 3-orbital Hubbard model and some *ab initio* descriptions have been largely used and investigated within different schemes of approximation, providing possible interpretations for the phase diagram in $(\text{Sr,Ca})\text{RuO}$ systems.

There have been systematic Hartree-Fock studies to determine the most favorable phases with respect to the multiplet interaction parameters and the electron-lattice coupling.^{6,23–25} Although the Hartree-Fock method has the advantage of simplicity and reliability, especially when correlation effects are not strong, many attempts have been performed for going beyond this approximation.

To capture the correlation effects associated with the Mott metal-insulator transition, the dynamical mean-field method (DMFT) has been applied to such class of systems.²⁶ In this frame, due to the presence of the orbital degrees of freedom, the Mott physics contains extra elements of unconventional character. Studies in this direction have indicated the possibility of orbital selective Mott transitions in reduced multi-orbital models, showing that separate Mott transitions occur at different Coulomb strengths, eventually merging into a single critical point only for special conditions²⁷ even though the debate on the phenomenology of the Mott physics in this type of system is still under study.^{28,29} An unbiased scheme of computation on small size systems has been used to investigate the nature of the spin/orbital correlations in the different regimes of microscopic couplings.³⁰ Despite the fact that this analysis is restricted to limited size clusters, the results obtained are interesting since it has been shown that short range patterns with a new type of orbital distribution with a doubling of the unit cell in the plane may occur. This configuration has been considered to comprehend the occurrence of G-type antiferromagnetism in a state with partial filling of the xy band, for the case of the Ca_2RuO_4 compound.

In conclusion, the phenomenology of these materials is rather complex since it is the result of the competition of many degrees of freedom. Moreover, the presence of several energy scales makes it difficult to establish the most favorable spin/orbital configuration of the ground state. For this reason, in this paper we concentrate on the problem of the evolution of short range quantum correlations as a function of the different interactions relevant at a microscopic level. In particular, we consider an extended version of the 3-orbital Hubbard model on two effective t_{2g} sites in an octahedral environment. This basic case is investigated by means of exact diagonalization techniques, where all the pos-

sible local correlated features are included and the three-dimensional connectivity for the t_{2g} orbitals is projected on one effective bond. This projection procedure allows us to simulate a *real* system with one t_{2g} site connected with three *locally* equivalent sites along the crystallographic directions. While on each bond there are only two active hoppings among the t_{2g} orbitals, by taking the neighbors sites as equivalent, one may replace the result of the charge transfers due to the surrounding, via an effective one-site environment. Hence, the analysis of one effective bond, with all the homolog orbitals connected via a single particle hopping, can, on average, simulate one t_{2g} site embedded in a three-dimensional environment whose feedback of the charge fluctuations along all the directions is included. In this way, the symmetry is not broken explicitly and the information of the directional electron transfer is contained in the correspondent connectivity of each orbital in the t_{2g} sector. Therefore, the occurrence of a specific spin/orbital pattern on the bond upon examination would refer to a situation where there is an isotropic exchange along the three crystallographic directions.

Specifically, we will address the following questions: (i) the competition between the charge fluctuations induced by the Coulomb repulsion and those due to the crystalline field energy associated with flat or elongated octahedra; (ii) the role played by the spin-orbit in modifying the configurations stabilized by the Coulomb repulsion and the tetragonal distortions; (iii) the effect of a spin polarizing field in controlling the magnetic and orbital correlations. Concerning question (i) and referring this point to the ruthenates oxides, we notice that, for the single layered Ca_2RuO_4 , we will investigate the transition from an antiferromagnetic ground state in a flat octahedral environment to a ferromagneticlike state for elongated octahedral configurations. This changeover can be induced both by applying an external pressure or via a suitable chemical substitution ($\text{Ca}_{2-x}\text{Sr}_x\text{RuO}_4$). In our analysis, we show that only in a suitable regime of Coulomb strength versus the crystal field potential, is it possible to drive the ground state from an antiferromagnetic to a ferromagnetic configuration. Referring to question (ii), we discuss the charge orbital distribution in the Ca_2RuO_4 compound. In particular, we analyze how the spin-orbit interaction in the presence of flat distortions is able to stabilize the antiferromagnetic ground state with predominantly ferrolike orbital correlations and a partial filled charge distribution in the xy orbital sector. As far as question (iii) is concerned, our study may provide some indications on the tendency of the system to develop antiferro-type orbital correlations under an external magnetic field starting from a nonpolarized configuration with a disordered orbital pattern. This feature may have some interest when referred to the bilayered $\text{Ca}_3\text{Ru}_2\text{O}_7$ system. Indeed, a possible scenario for the CMR phenomenon is related to the idea that polarizing spins stabilizes the orbitally ordered state, while an unpolarized state yields a melting of the orbital order.

The outline of the paper is the following: in Sec. II we present the microscopic model. Section III is devoted to the investigation of the phase diagram in presence of pure local Coulomb correlations and crystalline field. In Sec. IV, the coupling between spin and orbital dynamics is introduced and analyzed in the case of an environment with distorted

octahedra. Finally, Sec. V is devoted to the effects induced by a magnetic field on the ground state properties. Section VI contains a summary of the results and the concluding remarks.

II. THE MODEL

The model Hamiltonian we refer to is built up by different contributions that reproduce the complex local dynamics of electrons in the t_{2g} manifold,

$$H = H_{\text{kin}} + H_{\text{el-el}} + H_{\text{cf}} + H_{\text{so}}. \quad (1)$$

We point out that, in the present effective model, the electron variables of the oxygens have been projected out and we limit ourselves to the pure dynamics of the $4d$ bands.

The first term in Eq. (1) is the kinetic operator that defines the connectivity between the t_{2g} orbitals through the oxygen ions,

$$H_{\text{kin}} = -t \sum_{ij,\sigma} (d_{i\alpha\sigma}^\dagger d_{j\alpha\sigma} + \text{H.c.}), \quad (2)$$

$d_{i\alpha\sigma}^\dagger$ being the creation operator for an electron with spin σ at the i site in the α orbital. The hopping amplitude is assumed to be t for all the orbitals in the t_{2g} manifold, due to the symmetry relations of the connections via oxygen π ligands. Of course, being limited to an effective two-ions system, the hoppings along all the directions are projected on one bond.

The second term in H stands for the local Coulomb interaction between t_{2g} electrons,

$$H_{\text{el-el}} = U \sum_{i\alpha} n_{i\alpha\uparrow} n_{i\alpha\downarrow} - 2J_H \sum_{i\alpha\beta} \mathbf{S}_{i\alpha} \cdot \mathbf{S}_{i\beta} + \left(U' - \frac{J_H}{2} \right) \sum_{i\alpha\beta} n_{i\alpha} n_{i\beta} + J' \sum_{i\alpha\beta} d_{i\alpha\uparrow}^\dagger d_{i\alpha\downarrow}^\dagger d_{i\beta\uparrow} d_{i\beta\downarrow}, \quad (3)$$

where $n_{i\alpha\sigma}$, $\mathbf{S}_{i\alpha}$ are the on site charge for spin σ and the spin operators for the α orbital, respectively. U (U') is the intra (inter) orbital Coulomb repulsion, J_H is the Hund coupling, and J' the pair hopping term. Due to the invariance for rotations in the orbital space, the following relations hold: $U = U' + 2J_H$, $J' = J_H$.

The H_{cf} part of the Hamiltonian H is the crystalline field, controlling the symmetry lowering from cubic to tetragonal one,

$$H_{\text{cf}} = \Delta \sum_i (n_{i_{xy}} - n_{i_{xz}} - n_{i_{yz}}). \quad (4)$$

Positive (negative) values of Δ are related to elongated (flat) RuO_6 octahedron along the c axis and favor the occupation in the $d_{\gamma z}$ (d_{xy}) sector, respectively. It is worth mentioning that in this description the microscopic parameter Δ contains both the contribution for symmetry lowering due to the static Coulomb potential of the surrounding oxygens and the energy shift due to the formation of antibonding molecular orbitals between the transition metal atom and the neighbors oxygens.

Finally, having in mind the physics of electron correlations in ruthenate oxides, it is important to consider also the

spin-orbit coupling within the t_{2g} manifold. Since the spin-orbit interaction in the $4d$ shell is relevant, the orbital angular momentum L can strongly couple to the spin. We introduce thus the local orbital operator for the total angular momentum $\mathbf{L}_i = (L_{ix}, L_{iy}, L_{iz})$, whose components can be expressed in terms of the orbital fermionic operators,

$$L_{iz} = i \sum_{\sigma} [d_{i_{yz}\sigma}^\dagger d_{i_{xz}\sigma} - d_{i_{xz}\sigma}^\dagger d_{i_{yz}\sigma}],$$

$$L_{ix} = i \sum_{\sigma} [d_{i_{xz}\sigma}^\dagger d_{i_{xy}\sigma} - d_{i_{xy}\sigma}^\dagger d_{i_{xz}\sigma}],$$

$$L_{iy} = i \sum_{\sigma} [d_{i_{yz}\sigma}^\dagger d_{i_{xy}\sigma} - d_{i_{xy}\sigma}^\dagger d_{i_{yz}\sigma}]. \quad (5)$$

The Hamiltonian for the spin-orbit interaction is then written as

$$H_{\text{so}} = \lambda \sum_i \mathbf{L}_i \cdot \mathbf{S}_i, \quad (6)$$

where λ is the coupling constant.

III. INTERPLAY BETWEEN COULOMB CORRELATIONS AND CRYSTAL FIELD POTENTIAL

As first target, we have investigated the interplay between the Coulomb correlations and the local crystal field amplitude, looking at ground state phase diagrams. The results for this case and for the subsequent analysis refer to the two-site system with a total amount of 4 electrons in the t_{2g} sector for each site at zero temperature.

Hereafter, in order to have a quick reading of the phase diagrams, we introduce the following notation: A/B (m, k, l) stands for a magnetic/orbital A/B pattern with on-site charge distribution for orbital given by $\langle n_{i_{xy}} \rangle = m$, $\langle n_{i_{xz}} \rangle = k$, $\langle n_{i_{yz}} \rangle = l$; whereas we use the notation (m, k) one refers to a situation with equal charge occupation in the two orbitals of the γz sector. F, AF, C indicate ferromagnetic, antiferromagnetic, and canted spin arrangement, respectively. FO, AFO, OD stand for ferro-orbital (double occupation on neighbors homolog orbitals), antiferro-orbital (double occupation on neighbors off-diagonal orbitals), and orbital disorder correlations (quantum superposition of diagonal and off-diagonal orbital correlations).

Let us then discuss the competition between the electronic correlations and the static octahedron deformations simulated via the parameter Δ . The results are summarized in Figs. 1 and 2. We have reported the outcome of the numerical analysis by means of an exact diagonalization technique for (i) the fully degenerate case ($\Delta=0$) in the parameter plane $[J_H/t, (U'-J_H)/t]$ and (ii) as a function of the crystal field amplitude by keeping fixed the ratio J_H/U' , in a way that at $\Delta=0$ all the regions of the case (i) can be reached by varying $(U'-J_H)/t$.

Case (i) allows for the study of the interplay between Hund's coupling and Coulomb interaction for the case of homogeneous charge occupation due to the complete orbital degeneracy. One can observe that the competition between

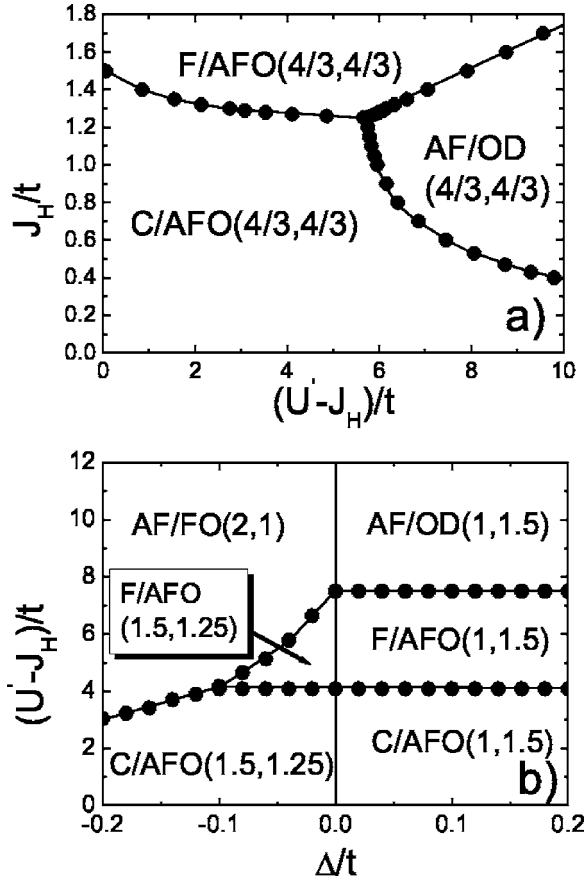


FIG. 1. Phase diagram at zero temperature for (a) the triple degenerate case and (b) as a function of the crystal field amplitude.

Hund and Coulomb repulsion generates a phase diagram with three distinct regions. Below a critical value of J_H and U' , the interplay between local ferromagnetic correlations and antiferro-type exchange due to the Coulomb repulsion, brings the system toward an incomplete ferromagnetic configuration (C) with off-diagonal orbital correlations between double occupied orbitals (AFO). The magnetic character of the ground state is extracted by looking at the evolution of the average local $\langle S_i \cdot S_i \rangle$ and off-site spin correlator $\langle S_i \cdot S_j \rangle$. In particular, it is possible to deduce the following magnetic behavior: full alignment in a triplet configuration on each site, indicated by the maximum allowed local spin-spin correlations compatible with the charge dis-

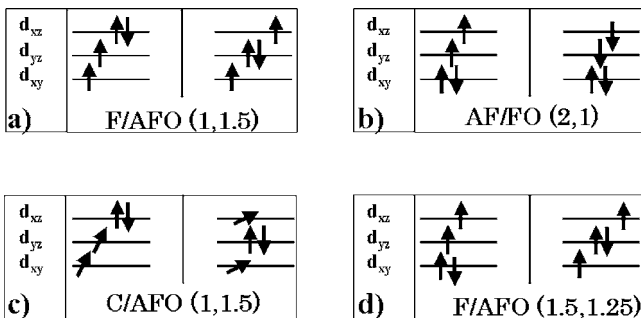


FIG. 2. Schematic representation of possible ground states for the two corner sharing octahedra system.

tribution, and incomplete antiferromagnetic correlations on neighbor sites, that leave out a total magnetic moment of $1 \mu_B$. On the other hand, to extract the off-site distribution of double occupied configurations, we look at the equal-time correlator $\langle D_{i\alpha} D_{i\beta} \rangle$ evaluated on the ground, where $D_{i\alpha} = n_{i\alpha\uparrow} n_{i\alpha\downarrow}$. Its amplitude indicates the tendency of the two-particles state to occupy homolog and/or different orbitals on neighbor sites. By monitoring these correlation functions it is possible to infer that the main part of the ground state is represented by a configuration of the form schematized in Fig. 2(c).

For large J_H/t the C/AFO evolves in a saturated ferromagnetic state, still in a configuration with now more robust AFO correlations also imposed by the Pauli principle. On the other hand, by increasing the value of U' (U) it occurs a transition to an antiferromagnetic ground state without any preference for the correlations between doubly occupied configurations on different sites, a state that we have indicated as orbital disordered (OD).

The crystal field potential suitably controls the relative concentration between d_{xy} electrons and the d_{yz} ones, as it couples directly to the difference between their densities. We will see that, depending on the sign of its amplitude, there occurs a redistribution of the charge between the t_{2g} orbitals, that turns out to be relevant for the magnetic and orbital character of the ground state.

Irrespective of the coupling strength, for positive values of Δ , it occurs as an average orbital occupation of $\langle n_{ixy} \rangle = 1$, $\langle n_{ixz} \rangle = \langle n_{iyz} \rangle = 1.5$. The relative phase diagram is reminiscent of the degenerate case (i). Indeed, the line of transition from one region to another is practically unaffected by the presence of Δ . This is due to the fact that, by lowering the energy of the γz sector, the orbital degeneracy is still active for the double occupied configuration which cannot be fixed in one orbital state. Still, the breaking of orbital symmetry by an arbitrary small positive Δ yields a sudden jump in the density distribution from the homogeneous case $4/3$ for the three orbitals to that with $(n_{xy}, n_{yz}) = (1, 1.5)$. For negative values of Δ , the energy lowering of the d_{xy} orbital with respect to the d_{yz} would favor a freezing of this degree of freedom in a doubly occupied configuration, that is then magnetically inert. The remaining part with half-filled d_{yz} orbitals, via a cooperation of Hund and superexchange, gives rise to antiferromagnetic correlations via spin one objects. Due to the favorable gain both in the crystal field and potential energy, such state tends to dominate the negative side of the phase diagram with respect to the partial (C/AFO) and total polarized state (F/AFO). Higher values of Δ requires a smaller intersite Coulomb repulsion to stabilize the AF/FO(2,1) ground state.

It is interesting to look in more detail at the transition between the AF/OD(1,1.5) and the AF/FO(2,1). Due to a peculiar character of the ground state and of the intermediate configurations introduced by the pair hopping processes, the change in the orbital distribution occurs without abrupt jumps, but via a continuous transfer of charge among the different orbitals in the t_{2g} manifold.

It is worth stressing that the interplay between static octahedron deformation, via the crystal field, and the Coulomb

interaction yields a complex variety of behaviors concerning the short range CSO correlations. As a summary of the outcome, one can observe that in general there is an occurrence of AFO correlations with noninteger orbital occupation and polarized states, while the orbital pattern for the antiferromagnetic state turns out to be strongly dependent on the character of the deformation. Moreover, the ferromagnetic correlations are strongly suppressed by the flat octahedron, while elongated configurations tend to not be destructive with respect to the polarized configuration.

This aspect is relevant when one is referring to the case of the ruthenates oxides. As discussed in the Introduction, the single layered Ca_2RuO_4 ruthenate has an octahedral structure at low temperature where the distance between the Ru atom and the in-plane oxygens (Ru-O[1]) is larger than that with the apical oxygen (Ru-O[2]). By means of chemical substitution and external pressure, it is possible to drive a structural changeover in the ratio between the apical and the in-plane Ru-O lengths. Indeed, at a critical concentration of Sr in the $\text{Ca}_{2-x}\text{Sr}_x\text{RuO}_4$ compound there is a transition where the ratio in the octahedral distances modifies yielding a change from a flat to an elongated structure.¹⁷ Similarly, the pressure stabilizes the low volume phase inducing a phase transition from a flat to an elongated octahedral configuration.^{19,20} The consequent variation of the Ru-O distances is generally associated with a modification in the magnetic and transport properties. Indeed, the transition from flat to elongated structure is linked to that from an antiferromagnetic insulator to a ferromagnetic (partial polarized) metallic state.

In this respect, our results describe how the effects of the crystal field potential are able to tune the AF/FO state into a weakly/strongly polarized configuration. It turns out to be crucial for such scenario to be in a suitable regime in the space of Coulomb parameters. Indeed, only below a critical threshold for $U'-J_H$ it is possible to drive the AF state into a F or C-type state. The suppression of charge fluctuations, due to the Coulomb repulsion, leads to a transition into a fully polarized configuration even for a small degree of flattening along the c axis.

IV. COUPLING BETWEEN SPIN AND ORBIT IN THE PRESENCE OF OCTAHEDRAL DISTORTIONS

Let us consider now the interplay between the spin-orbit interaction and the octahedron distortions and their effects on the correlated ground state.

The main effect of the spin-orbit coupling is to allow for a rearrangement of the charge and spin giving rise to a local nonzero angular momentum linked to the direction of the local spin polarization. Due to its expression, \mathbf{L} tends to mix different orbitals, as an effective hybridization, forming the local basis for the single particle states of the type $|\psi_\gamma\rangle \sim |xy\rangle \pm i|\gamma z\rangle$ or $|\psi_z\rangle \sim |xz\rangle \pm i|yz\rangle$. For this system, we will see that there is a partial unquenching of the orbital degree of freedom, which is peculiarly linked to the orbital occupation. Indeed, as a consequence of the crystal field potential, the relevant component of the angular momentum will depend on the way the charge distributes on the different orbitals.

Hence, it turns out that the spin degrees of freedom, whose character at first is isotropic due to the spin-invariant local correlations, link to the orbital part.

In our case, there are two holes in the t_{2g} sector to rearrange as a function of the character of the octahedral deformation. If the octahedra are compressed ($\Delta < 0$), one has two possible local charge distributions, depending on the magnetic character of the ground state: (2,1) and (1.5,1.25). In the case (2,1), there is one hole in the xz and one in the yz orbital, respectively. Thus, it is natural to infer that the spin-orbit coupling would favor a configuration with one hole in the $|\psi_x\rangle \sim |xy\rangle + i|xz\rangle$ ($|\psi_y\rangle \sim |xy\rangle + i|yz\rangle$) and one in the $yz(xz)$ orbital state, respectively. Hence, the orbital and spin angular momentum will be aligned along the $x(y)$ direction. The situation with (1.5,1.25) corresponds to the case of 0.5 holes in the xy orbital and 1.5 in the γz , respectively. This circumstance has the same status of the previous one concerning the spin-orbit effect, with different weight in the quantum superposition due to the noninteger hole distribution. Still, it permits us to have spin and orbital angular momentum in the xy plane.

When the octahedra are elongated ($\Delta > 0$), the orbital occupation is given by (1,1.5), namely, on average there is one hole in the xy and one in the γz orbital, respectively. Due to the gain in crystal field energy for the γz sector and to the allowed processes of mixing via L_z , it is favorable to stabilize a configuration where the hybridization of these orbitals forms a state with one hole in the $|\psi_z\rangle \sim |xz\rangle \pm i|yz\rangle$ and leaving the other one in the quenched xy orbital. In this state, L and S angular momentum are directed along z . At this point one is left with the more complicated analysis of how the Coulomb correlations interfere with the formation of this local configuration and which types of nonlocal spin correlations are stabilized.

Let us now consider the question related to the interplay with the Coulomb correlations. We have seen in Sec. III that the crystal field potential, depending on the strength of the local Coulomb potential, is able to modify the orbital character of the antiferromagnetic state, and to separate regions with most favorable ferromagnetic correlations from others where antiferromagnetism is dominant. Now, we are interested in investigating how the Coulomb correlations interfere with the formation of locked spin and orbital momentum states. As in the preceding cases, to explore the possible ground states in the space of the microscopic parameters, we have chosen a ratio of J_H/U' in a way that the variation of $(U'-J_H)$ allows us to span all the regions of the diagram in Fig. 1.

A. Compressed octahedra

We analyze the case of flat octahedra with a representative value of the crystalline field equal to $\Delta/t = -0.15$. The phase diagram is reported in Fig. 3. There are three critical boundaries that separate the regions at zero spin-orbit coupling from those at finite λ . The boundary delimited by filled circles indicates a discontinuous change in the ground state accompanied by a jump in the related correlation functions. The curves marked by the crossed points and by the stars

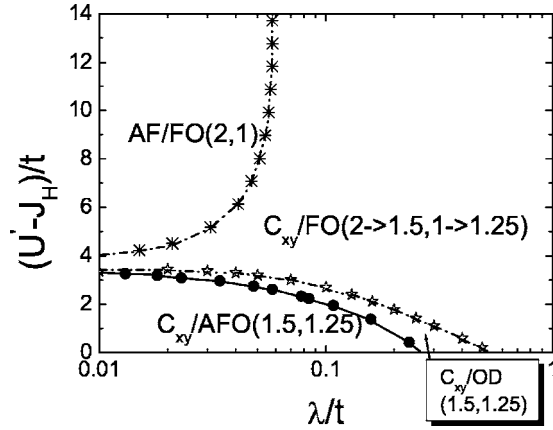


FIG. 3. Phase diagram as a function of the spin-orbit coupling λ/t for a crystal field amplitude $\Delta/t = -0.15$.

stand for a crossover between the quantum states, with a continuous behavior of the correlation functions. The points are taken in the positions where the correlators have a maximum change in the variation of their evolution as a function of λ .

Let us start from the $C/AFO(1.5,1.25)$ state at zero spin-orbit coupling, where off-site spin-correlations are antiferromagnetic like with configurations that allow for a nonzero isotropic total spin momentum, while the orbital correlations have large off-diagonal amplitude in the channel of double occupied correlators. The switch of the spin-orbit interaction produces a sudden removal of the rotational spin invariance, in a way that now the magnetic correlations are antiferromagnetic but stronger in the xy plane ($\langle S_i^{x,y} S_j^{x,y} \rangle$) than along the z direction ($\langle S_i^z S_j^z \rangle$), where the ferromagnetic moment mainly manifests. This is a consequence of the tendency in forming orbital configuration with two holes in the $|\psi_x\rangle \sim |xy\rangle + i|xz\rangle$ ($|\psi_y\rangle \sim |xy\rangle + i|yz\rangle$) and $yz(xz)$ orbitals, respectively. The total spin momentum turns out to be anisotropic in this region with larger amplitude in the z direction. Furthermore, due to the orbital dependent charge distribution, the main part of the spin correlations are derived from the γz sector.

At a critical value of λ , whose amplitude decreases as the electron correlation ($U'-J_H$) increases, the system exhibits two transitions. First, it changes into a C_{xy}/OD state and then it smoothly crosses over in a C_{xy}/FO . The main modifications do not occur in the spin channel, because both the ending regions are characterized by off-site spin correlations that are more antiferromagneticlike with respect to the $C/AFO(1.5,1.25)$ and prevalently in the xy plane, with a small net magnetic moment along the z direction, which is reminiscent of the local spin invariance of the Coulomb correlations. In the orbital part, by looking at the correlator between double occupied configurations, one can observe a redistribution of charge that strongly renormalizes the off-diagonal orbital channel leading first to a disordered configuration and then, at larger spin-orbit coupling, to more pronounced diagonal amplitude giving a substantial FO character to the ground state. In other words, the system evolves in a configuration where the double occupation is mainly in the $|\psi_x\rangle \sim |xy\rangle + i|xz\rangle$ ($|\psi_y\rangle \sim |xy\rangle + i|yz\rangle$) with unequal weight

for the projection on the xy orbital with respect to the γz ones. This aspect is a consequence of the crystal field splitting that does not favor having much charge concentrated in the γz sector.

Moreover, due to the increase of antiferromagnetic correlations with respect to the C_{xy}/AFO state, there is a reduction of the total spin momentum (weak ferromagnetism) that is still different from zero and anisotropic. Another crucial aspect is represented by the fact that the charge occupation in this region changes as a function of λ in a continuous way towards a value of $\sim(1.5, 1.25)$ reaching the strong coupling limit. Such a feature is related to the tendency of the spin-orbit coupling towards the mixing of xy with the γz orbitals. The quantum superposition which emerges, on the other hand, cannot allow for an equal charge population in the two sectors due to the crystal field potential. Hence, there occurs a competition which manifests as a gradual charge transfer between the two parts of the t_{2g} manifold as the spin-orbit coupling is compared to the crystal field energy.

It is also peculiar how, in the limit of strong coupling and compressed octahedron distortion, the ground state evolves as a function of the spin-orbit coupling. Indeed, it turns out that all the correlators change in a continuous way from AF/FO to C_{xy}/FO . The smooth character of the correlator may be linked to the small change in the orbital part, which is just characterized by a weakening of FO correlations due to the presence of small off-diagonal contributions, although the dominant aspect remains of the FO type. All the main transformations occur in the spin channel. We have to remind that the AF/FO has zero spin angular momentum and isotropic antiferromagnetic correlations. The introduction of the spin-orbit coupling makes the system staying magnetically isotropic until, at the crossover points, it changes by evolving into the C_{xy}/FO , where the antiferro-type correlations keep almost the maximum value in the xy plane (still there is a small ferromagnetic net momentum), while tend to quench along the z direction. The freezing of superexchange mechanisms along the z direction is accompanied by a formation of weak ferromagnetism. It is worth pointing out that the position of the crossover becomes quite insensible to the change in Coulomb correlations above a critical value, while it has a quick activation from zero coupling to finite value in the intermediate regime of $U'-J_H$. Indeed, there is a point at $\lambda = 0$ and $(U'-J_H)/t \sim 4$, where the system goes from FO to AFO configurations. Hence, it does happen that in this region those states are almost degenerate in energy. It is then the effect of orbital hybridization of the spin-orbit coupling that links those configurations determining a slight weakening of FO correlations. The same process occurs also in the spin channel, being strongly correlated to the orbital one. Indeed, the mixing of the orbital basis induces also a superposition of C and AF which then yields the C_{xy} configurations.

In conclusion, as far as the case of compressed octahedron in the presence of spin-orbit coupling is concerned, we have seen that the correlated ground state is quite sensible to this interaction. In particular, the FO configuration, where the xy orbital is quenched, smoothly evolves to a state with not integer orbital population, whose xy occupation is not completely quenched.

It is then worth pointing out that the phase diagram is dominated by a large region where the orbital correlations

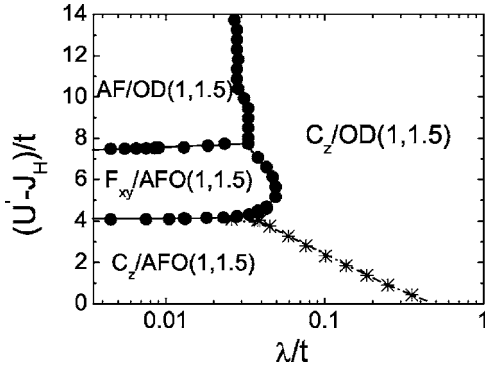


FIG. 4. Phase diagram for different $U'-J_H$ as a function of the spin-orbit coupling λ with positive crystal field amplitude $\Delta/t=0.15$.

are ferro-type with a not-integer occupation of the different sectors of the t_{2g} manifold. These results can shed light into the debate about orbital distribution in CaRuO systems. Particularly, we emphasize the correspondence with what was found in Ref. 6 for the Ca_2RuO_4 compound, where the existence of an orbital configuration having two holes in the yz and $|\psi_\gamma\rangle \sim |xy\rangle \pm i|\gamma z\rangle$ orbitals, L and S momenta being directed along the x or the y axis, is attributed to the cooperation between the small compression of the RuO_6 octahedra and the strong spin-orbit coupling. Our calculations in the flat configuration in presence of the spin-orbit coupling, give a simple explanation of the previous observation including the aspect of having 0.5 holes in the d_{xy} orbital sector.

B. Elongated octahedra

We take in exam one representative situation with positive amplitude of the crystal field given by $\Delta/t=0.15$, the phase diagram being reported in Fig. 4. For this situation, the cross-over from rigid orbital patterns to OD occurs in the weak coupling part of the phase space $(U'-J_H)/t \sim 2$, while the remaining spin-orbit induced transitions are all with an abrupt jump in the correlation functions. With respect to the compressed octahedron, the orbital average density turns out to be constant as the spin-orbit interaction varies. This is a consequence of the interplay between the removal of orbital degeneracy and the orbital charge distribution. Indeed, the application of a positive crystal field amplitude tends to collocate the double occupied configuration in the γz sector. Due to the energy splitting with the xy orbital, it is natural that the spin-orbit coupling is predominantly active only via L_z , yielding a superposition of xz and yz states that keeps the average occupation unchanged.

This possibility is interesting with respect to the previous one, as it permits us to study the full polarized state F/AFO under the perturbation of the spin-orbit coupling. Indeed, at arbitrary small λ , the isotropic ferromagnetic state evolves into a configuration F_{xy} where only the planar xy correlations keep the F character, while out of plane it is weakly antiferro-type. Such aspect can be extracted by the behavior of the correlator $\langle S_i^2 \rangle$ with $i=x, y, z$. It turns out that in the F_{xy} state the total spin momentum is completely aligned along

the xy direction, while along z has an amplitude of about zero, indicating more antiferrolike correlations. The state is stable up to a critical value of $\lambda/t \sim 0.05$, above which the ground has complete AF correlations along the z direction and weak ferromagnetism in the plane.

On a general ground, the effect of the spin-orbit interaction is strictly related to the character of the octahedron distortions. Orbital ordered configurations are stabilized in the flat case with respect to the compressed one, where there is no preferential double occupation in the γz sector. Concerning the magnetic channel, the orbital hybridization induced by the spin-orbit mechanism allows for a combination of F and AF-type states for giving a C-type configuration. Such ground state has easy-axis antiferrolike correlations in the plane of orbital angular momentum, while the weak ferromagnetic component manifests in the perpendicular direction.

V. RESPONSE TO A SPIN ONLY COUPLED MAGNETIC FIELD

In this section, we are interested in probing the response of the system to a magnetic field both along and perpendicularly to the direction of the easy-axis magnetization, limiting ourselves to the consequences of a pure spin coupling. The interaction between the external field and the local moment can be expressed as

$$H_{sf} = - \sum_i \mathbf{B} \cdot \mathbf{S}_i, \quad (7)$$

where \mathbf{B} is the vector magnetic field in units of Bohr magneton, and \mathbf{S}_i is the local spin moment.

As we have discussed in the Introduction, the present analysis can be interesting in connection with the case of magneto-transport phenomena observed in the $\text{Ca}_3\text{Ru}_2\text{O}_7$ system. Though our results are limited by the small size of the cluster under analysis, they may be taken as a building block for getting more insight in the evolution of short range correlations when a field is applied to the compound above mentioned.

As a general target, we investigate how the charge and orbital configurations rearrange as a consequence of polarizing the spin along a specific direction. We have seen in the previous sections that the spin/orbital/charge correlations are intimately connected. Moreover, the degree of interrelation manifests differently depending on the distortion of the octahedron and on the spin-orbit strength. For this reason, we expect that the effects of spin polarization influence the ground state in a nontrivial way, inducing competing charge/orbital patterns. Since one is dealing with many parameters, the adopted strategy is to start from a configuration with nonzero $\lambda/t=0.2$ and $\Delta=\pm 0.15$ and then to study the changes of the ground state both as a function of the magnetic field and of the Coulomb correlations. The ratio between the Hund coupling and the Coulomb repulsion is the same as that of the phase diagram in Fig. 1.

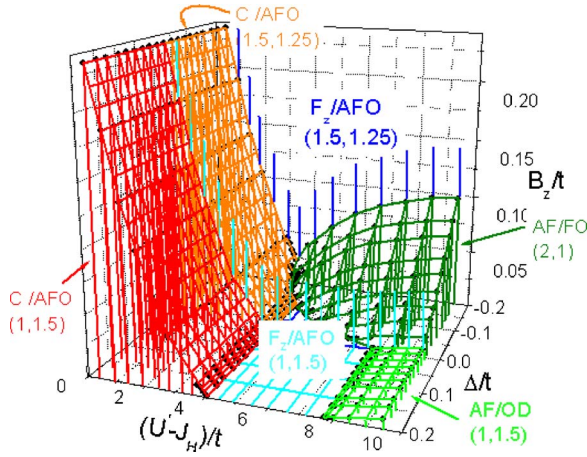


FIG. 5. (Color online) Phase diagram as a function of the external field, the Coulomb parameters U' and J_H , and the crystalline field amplitude at zero spin-orbit and Jahn-Teller coupling.

A. Response to a magnetic field without spin-orbit and in presence of octahedral distortions

In Fig. 5 we have reported the evolution of the boundaries determined in Fig. 1 under the application of a spin only field. We notice that the choice of the z axis is not relevant in this case since all the directions are equivalent in absence of spin-orbit coupling.

As expected, all the regions shrink as the amplitude of the field increases, except the fully polarized phase region (F_z/AFO) that extends over almost all the phase space. We notice that the response is highly dependent on the strength of the Coulomb interaction, and on the character of the octahedral distortions. Indeed, in the weak/intermediate-coupling limit [$(U'-J_H)/t < 5$], the two canted configurations show the same behavior under the effect of an external field, independently of the nature of the distortions and the orbital distribution. One can observe that, to overcome the tendency towards a paramagnetic configuration, the amplitude of the field has to get larger and larger as the strength of the Coulomb parameter decreases. This is a consequence of the fact that in this limit the kinetic energy is comparable with the potential one and there are paramagnetic local two-particle states that make more difficult the formation of a polarized state. The relevant scale of energy in this case is represented by the absolute ratio $(U'-J_H)/t$.

When the charge fluctuations start to get suppressed, we have already seen that the system manifests an asymmetry in the ground state properties, which is strongly dependent on the type of octahedral distortions. In the intermediate/strong coupling limit [$5 < (U'-J_H)/t < 8.5$], the elongated octahedra is dominated by a fully polarized ground state, while the flat case shows a tendency towards antiferromagnetic correlations with ferro-type orbital order. Of course, the field does not modify the nature of the F_z state, while the AF/FO gets destabilized, in a way that the intensity of \mathbf{B} required has to grow almost proportionally to the amplitude of the crystalline field. This is due to the need of a charge transfer from the lowest xy orbital to the γz manifold when one moves from the AF/FO to the AF/AFO configuration. Such a pro-

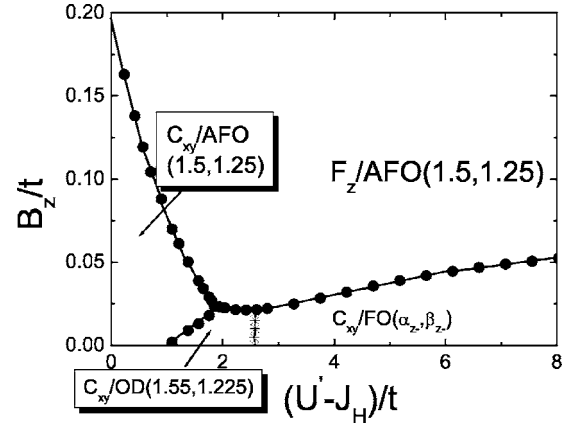


FIG. 6. Phase diagram as a function of the magnetic field along the z direction for a representative so coupling $\lambda/t=0.2$ and a crystalline field amplitude $\Delta/t=-0.15$. The value α_{z-} refers to the average density $\langle n_{xy} \rangle$ and varies continuously in the range $[1.5, 2]$ as $U'-J_H$ increases. On the other hand, $\beta_{z-} = \langle n_{xz} \rangle = \langle n_{yz} \rangle$ changes as a function of $U'-J_H$ in the interval $[1.0, 1.25]$. The subscript $z-$ stands for magnetic field along z and negative value of the crystalline energy Δ .

cess has a cost in energy of about Δ . Furthermore, it is worth pointing out that there is no intermediate transition from the zero spin ground state (AF/FO) to the fully polarized configuration F_z .

The response of the AF/OD ground state, in the strong coupling limit with elongated octahedra, shows a completely different behavior. The boundary in the low field limit does not change substantially as a function of Δ , showing that the exchange processes are independent on the strength of the distortions. In this case the relevant scale of energy, which controls the transitions between the AF and F state, is related to the orbital exchange in the γz sector.

B. Compressed octahedra with magnetic field perpendicular to the easy axis B_z

For a flat octahedral distortion, the outcome of the response to a spin only field applied perpendicularly to the easy axis is reported in Fig. 6. As one can observe, the main consequence of the spin polarization along the z direction is to induce an extra region with respect to the case at zero field and to enlarge the portion of stability of the phase C_{xy}/AFO (1.5,1.25) in the weak coupling limit. The new area is marked by a configuration with a complete polarization along the direction of the external field and with antiferrolike orbital correlations F_z/AFO (1.5,1.25). Let us start from the zero field situation. As discussed in Sec. IV, the cooperation of crystal field energy and Coulomb interaction induces a ground state where the $L_x(L_y)$ component are mainly active so that the spin correlations are predominantly in the xy plane and antiferrolike with a small magnetic moment in the z direction. Furthermore, one can see that, depending on the amplitude of $U'-J_H$, it is possible to tune the system from an AFO to an OD and then to a FO configuration, with a gradual redistribution of the charge between the γz sector and the xy orbital. These possibilities are reported in Fig. 7,

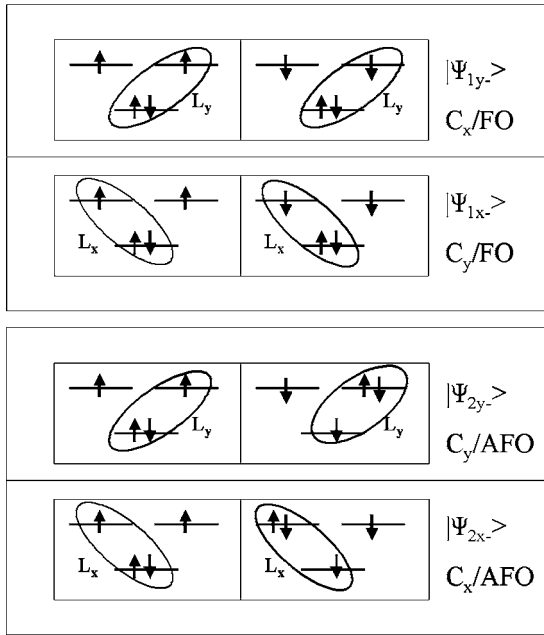


FIG. 7. Schematic representation of the two contributions to the ground state in the case of compressed octahedron for the C_{xy}/FO (upper panel) and C_{xy}/AFO (bottom panel), respectively. In this circumstance the lowest energy configuration is basically due to a quantum superposition of the states $|\psi_{1x-}\rangle(|\psi_{2x-}\rangle)$ and $|\psi_{1y-}\rangle(|\psi_{2y-}\rangle)$ for the C_{xy}/FO (C_{xy}/AFO). The circle around the xy and $xz(yz)$ orbitals indicates that the $L_x(L_y)$ part of the angular momentum is active and the double occupied configuration lives in a mixture of the two states, respectively.

where we have made a sketch of the representative contributions to the ground state in the different orbital arrangements. For the case of the OD state, one has to consider a quantum superposition of the case AFO and FO with comparable weight. A key feature of the cooperative spin-orbit and crystal field potential, is to have a ground state with main FO correlations between the xy orbitals, but with not integer orbital occupation.

The application of the field along the z direction has two main consequences: (i) in the spin channel, it occurs a transition to a fully polarized state as expected; (ii) in the charge/orbital channel, the polarization along z freezes the spin-orbit contribution $\sim L_{x(y)} \cdot S_{x(y)}$ that was responsible for the no integer orbital population in the xy and γz sectors. Aspect (ii), together with the Pauli principle, that forces the ground state to avoid single occupied configurations on homolog orbitals, yield a charge distribution with $\langle n_{xy} \rangle = 1.5$ and $\langle n_{xz} \rangle = \langle n_{yz} \rangle = 1.25$ with AFO.

Looking at lower values of Δ , one observes a shift in the transition point to smaller magnetic field amplitudes, thus revealing the competition between the crystalline and magnetic energy in stabilizing a polarized state.

C. Compressed octahedra with magnetic field parallel to the easy axis $B_{x(y)}$

The phase diagram for the case with a field applied in the plane along the x axis is reported in Fig. 8. The regions that

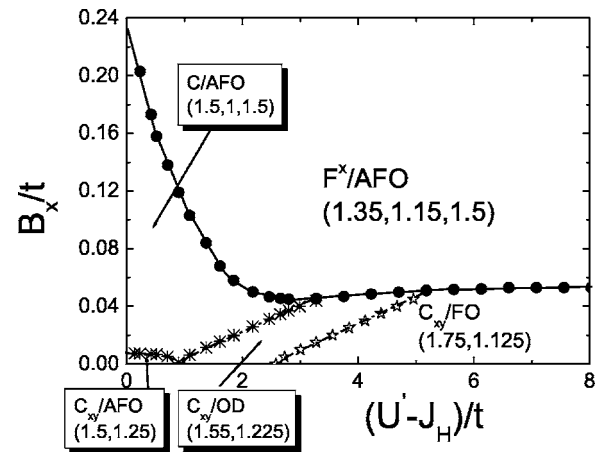


FIG. 8. Phase diagram as a function of the magnetic field along the x direction for a representative so coupling $\lambda/t=0.2$ and a crystalline field amplitude $\Delta/t=-0.15$.

appear at zero field evolve into a state that is completely polarized along the x direction and that has dominant anti-ferrolike orbital correlations (F_x/AFO). The behavior of the average charge distribution indicates that the double occupied configuration arranges as in Fig. 7, with the difference that now, due to the crystalline field energy, more charge accumulates in the xy orbital with respect to the xz . The density in the other orbital evolves in a way that allows for AFO correlations, so to optimize the gain in kinetic energy. There are a few aspects to underline.

The low field portion of the phase diagram is characterized by different lines of crossover between regions that are magnetically affine but present an occupation that allows for different orbital patterns. The line of crossover is a consequence of the competition between the crystal field, the spin-orbit coupling, and the magnetic field. Indeed, in the strong-coupling limit, where the charge fluctuations are suppressed, the attempt of optimizing the three competing mechanisms induces a crossover between different orbital arrangements. In particular, in the range of $U'-J_H$ between $\sim [2.5, 4.5]$, the application of the external field allows us to tune the orbital correlations from a FO to an OD type, before approaching the transition to the fully polarized state.

In the weak coupling limit of $(U'-J_H)/t$ within the range $\sim [1.0, 2.5]$, by growing with the amplitude of B_x , it is possible to change over from an OD configuration to an AFO one. The arrival state, that we indicated as C/AFO, manifests also an interesting magnetic pattern. Due to the anisotropy of the starting configuration C_{xy} , there is a partial recover of the rotational symmetry through the external field. The antiferromagnetic correlations are quantitatively comparable in all the directions. Still, there occurs a net spin moment in the x direction, while the fluctuations in the square of the magnetic moment also get comparable in all directions.

D. Elongated octahedra with magnetic field parallel to the easy axis B_z

Without the field, we have observed that the presence of a double occupation in the γz orbitals favors the local mixing

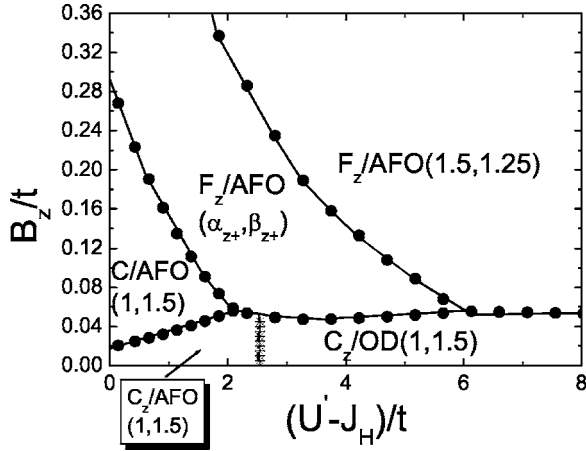


FIG. 9. Phase diagram as a function of the magnetic field along the z direction for a representative spin-orbit coupling $\lambda/t=0.2$ and a crystalline field amplitude $\Delta/t=0.15$. The value α_{z+} refers to the average density $\langle n_{xy} \rangle$ and varies continuously in the range $[1, 1.5]$ as the magnetic field increases. On the contrary, $\beta_{z+} = \langle n_{xz} \rangle = \langle n_{yz} \rangle$ changes as a function of B_z in the interval $[1.25, 1.5]$. The subscript $z+$ stands for magnetic field along z and positive value of the crystalline energy Δ .

of the xz, yz states via spin-orbit coupling and through the L_z component of the total angular momentum. Due to such quantum superposition, there are no specific tendencies in the character of the orbital correlations, having equally favored FO and AFO configurations in the γz sector. The spin pattern is anisotropic, with antiferromagneticlike correlations along the z direction (easy axis magnetization) and a residual small magnetic moment along the in-plane axis (x, y). The application of a field along the z direction modifies the ground state both in the orbital and spin sector as reported in the phase diagram of Fig. 9. We have to distinguish between two zones, below and above a critical value of $(U'-J_H)/t \sim 6$. In the former case, the instability of the C_z/OD (see Fig. 10), under the effect of the applied field, is accompanied by the formation of an intermediate state with incomplete polarization and AFO character, whose orbital occupation is not an integer but behaves as a superposition of two contributions with $(1, 1.5)$ and $(1.5, 1.25)$ orbital distribution. This is the result of the competition between the magnetic, spin-orbit, and kinetic energy. Indeed, once the polarization along

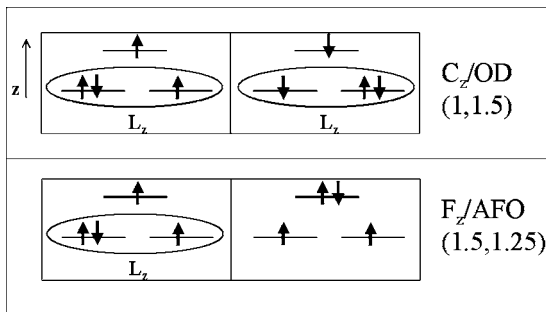


FIG. 10. Schematic representation of the main contributions to the ground state in the case of elongated octahedron and longitudinal magnetic field.

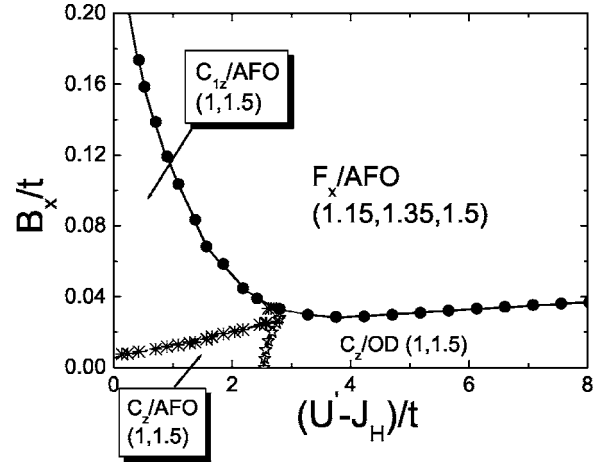


FIG. 11. Phase diagram as a function of the magnetic field along the x direction for a representative spin-orbit interaction $\lambda/t=0.2$ and a crystalline field amplitude $\Delta/t=0.15$.

the field gets in, it is preferable to avoid a connection between orbitals that are singly occupied. For this reason, it is more convenient to freeze the L_z orbital hybridization on one site, losing the correspondent crystalline field energy, while allowing a larger mobility for the double occupied objects. This optimizes the gain in kinetic energy. Such a configuration is schematically depicted in Fig. 10.

Another aspect that occurs in this region, and is typical of the weak-coupling regime $(U'-J_H)/t \sim 1$, is that the antiferromagnetic state is more stiff due to the large overlap between orbitals on different sites, thus to stabilize the fully polarized $F_z/AFO(1.5, 1.25)$ it required a field whose amplitude grows up to a scale of the order of the average kinetic energy. This is a consequence of charge fluctuations that get stronger in this regime (easy formation of double occupied intermediate state with zero spin momentum) and prevents the formation of a fully polarized configuration.

On the other hand, above the threshold $(U'-J_H)/t \sim 6$, there occurs a direct transition from the anisotropic antiferromagnetic state $C_z/OD(1, 1.5)$ to the fully polarized $F_z/AFO(1.5, 1.25)$ arrangement. It is worth noticing that the boundary line in this region is quite independent on the magnetic field and its scale of energy is smaller than (λ, Δ) . In this regime, due to the freezing of the charge fluctuations, it is enough to overcome the magnetic exchange energy to fully polarize the ground state. Moreover, since the AFO configurations are contained in the C_z/OD state, the orbital fluctuations are softer and more easily tunable in this transition.

E. Elongated octahedra with magnetic field perpendicular to the easy axis $B_{x(y)}$

In this case, the magnetic field couples to the x component of the spin moment, and thus tends to pin the angular momentum aligned in the same direction due to the presence of the spin-orbit coupling. By looking at the behavior of the relevant correlators, one can distinguish between four different regions (see Fig. 11). The low field portion of the phase

diagram is characterized by two possible ground states C_z/AFO and C_z/OD with the same orbital populations, that are separated by a crossover line indicating a smooth change over from one to another state as the Coulomb interaction grows (Fig. 11). This transition, is marked by a change in the local density, without modifying substantially the spin correlations, in a way that the off-diagonal orbital correlations occur with equal distribution of the diagonal one. The response of those configurations to a spin field polarized along x is completely different and depends on the amplitude of $U'-J_H$ though the magnetic character of the ground state is quite uniform in the whole range of Coulomb coupling.

As discussed in the previous sections, the C_z state has antiferromagnetic correlations along the z direction and a small net moment in the perpendicular one. In the weak coupling, there is a crossover line (crossed points) that separates two antiferromagnetic configurations C_z and C_{1z} with a different amplitude in the off-site correlator along the z direction. Increasing the field B_x weakens the antiferro-type correlations along z and induces a larger spin moment along x . However, as in the preceding case, the ground state is more stiff due to large charge and orbital fluctuations that extend also between the two sites.

By increasing $U'-J_H$, the instability of the C_z/OD state occurs for lower field amplitude, due to the softness of the antiferromagnetic configuration in the direction perpendicular to the easy axis once the charge fluctuations are suppressed in the ground state and the double occupied states appear only as virtual processes. Moreover, the transition from C_z/OD to F_x/AFO is accompanied by a peculiar redistribution of the charge. The activation of the L_x orbital component is responsible for the noninteger occupation in the xy, xz orbitals. The yz orbital state practically stays unaffected with respect to the external field. Concerning the orbital correlations, we observe an AFO pattern in the γz sector, as a consequence of the fully polarization of the spins in the x direction, so to avoid the double occupied diagonal configurations. It is worth pointing out that the final configuration F_x/AFO is a compromise in the balance between the crystalline energy and the spin-orbit coupling. The crystal field potential prevents the formation of double occupied configuration in the xy orbital. On the other side, due to the presence of a magnetic field along the x axis, the gain in the spin-orbit channel comes mainly from the term $\sim L_x \cdot S_x$. The competition between those two mechanisms, together with the gain by the magnetic field, yields a configuration with a superposition of active and inactive spin-orbit mixture of double and single occupied configurations between the xy orbital and the γz sector (see Fig. 12). Still, as a consequence of that, such quantum configuration manifests a noninteger orbital occupation.

VI. CONCLUSIONS

In conclusion we have explored the variety of ground state configurations that are generated in a system where various scales of energies, associated with the spin/orbital/lattice dynamics, are in competition. We have shown that, though limited to an effective two-site system within a

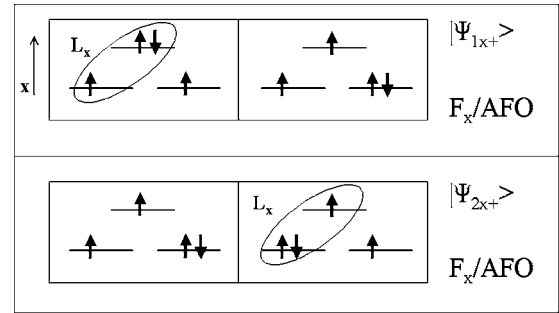


FIG. 12. Sketch of the main contributions to the ground state in the case of elongated octahedron and magnetic field along the x axis for the F_x/AFO region. In this case the lowest energy configuration is basically due to a quantum superposition of the states $|\psi_{1x+}\rangle$ and $|\psi_{2x+}\rangle$. The circles around the xy and xz orbitals indicate that the L_x part of the angular momentum is active and the double occupied configuration lives in a mixture of the two states.

$4d^4-t_{2g}$ manifold, it is possible to extract much information on the evolution of the short range correlations in the spin/orbital/lattice channel. The interplay between the Coulomb coupling and Hund exchange gives rise to different magnetic patterns depending on the relative strength of one interaction with respect to the other. In this frame, the spin configurations are marked by specific orbital correlations of the local two-particle states. Due to the peculiar filling under exam, it is the dynamics of the double occupied states that characterizes the orbital sector of the ground state. Generally, the spin polarized configuration are related to antiferro-type orbital correlations. The case of an antiferromagnetic ground state has more than one opportunity in the orbital channel.

Including the possibility of tuning the charge transfer between the xy and the γz sector via structural modifications (crystalline field potential) one can further control the occurrence of different patterns in the orbital and spin channel. It is quite interesting that a complete asymmetry in the magnetic response happens if one considers the flattened or elongated octahedral situation. Two different magnetic exchange mechanisms dominate in the negative or in the positive crystal field amplitude. In the flat case, the xy orbitals tend to be frozen as they are fully occupied, while in the γz sector the single particle states mediate an effective superexchange that yields a predominant antiferromagnetic ground state. On the other side, for an elongated octahedron, one observes a competition between a superexchange in the xy sector and a ferromagnetic exchange mechanism in the γz due to predominant AFO correlations. Indeed, the double occupation sits in the γz sector while xy orbital is single occupied. Thus, the gain due to orbital exchange polarizes the system and the spin in the xy sector too. When the superexchange between the localized spins in the xy sector overcomes the gain above mentioned, the antiferromagnetic ground state is stabilized.

As discussed in the Introduction, this asymmetric behavior has a correspondence with the experimental observation of the tendency towards an antiferromagnetic/ferromagnetic ground state in the flat/elongated octahedral configuration induced both via chemical substitution and applied pressure for the CaRuO family. This result underlines how the degree of flattening of the octahedra along the c axis is a key pa-

parameter in determining the magnetic and orbital correlations in the ruthenate oxides.

The analysis on the interplay between Coulomb repulsion and lattice distortions gives as outcome an integer or half-integer local average density for orbital. Such feature in the charge distribution is removed if one includes a coupling between spin and orbit. In this context, the ground state is strongly modified and it appears an interesting interplay between the spin/orbital pattern and the character of the octahedral distortions. In particular, the flatten(elongated) case in presence of a spin-orbit coupling favors the formation of anisotropic antiferromagnetic states with the magnetic moment lying along the direction of the correspondent and activated orbital momentum. Due to the local charge transfer induced by the orbital part of the spin-orbit coupling, the correlation between double occupied configurations tends to be disordered for the elongated case, in the sense that neither the ferro- nor the antiferro-type pattern is preferred, but a quantum superposition of the two cases. In the flatten octahedral configuration, the FO type of correlation persists but without a full occupation of the xy orbital, thus indicating the formation of an hybrid state with dominant FO configurations but with a still active charge dynamics in the xy sector. These results may be considered when one wants to address the question of the occurrence of an antiferromagnetic ground state in presence of flattening along the c axis with about 0.5 holes in the xy sector as it may occur in the Ca_2RuO_4 compound. The subtle interplay between the spin-orbit and the charge fluctuations controlled via Coulomb and crystal field potential turns out to be a key aspect in determining the spin and orbital character of the ground state.

Finally, we have presented how the orbital correlations are modified when the system gets spin polarized. Our analysis has been done along different directions with respect to the easy-axis polarization and for different structural conditions.

There is an interesting competition between spin-orbit, crystalline field potential and magnetic field. From a general point of view, when the strength of the external field is larger than the other scale of energies, all the electrons get spin polarized in a configuration with antiferro-type orbital correlations. What is different, depending on the direction of the applied field and on the octahedral deformation, is the path for reaching such state and the final charge distribution for each orbital. For example, in the flatten octahedra case, that is relevant for the CaRuO family of ruthenates, the FO correlations can be tuned to OD in the regime of a weak external field along the easy axis, inducing only a slight rearrangement of the spin structure. In this regime, the moments align roughly transverse to the applied field before gradually aligning along the field direction. Thus a kind of “flopping” of the moments from the easy to the hard axis naturally brings to a reorganization of the orbital distribution that in turn leads to an OD pattern.¹² On the other hand, when the field is applied perpendicularly to the easy axis, the FO correlations are more stiff and the ground state keeps its form until there occurs a transition to the AFO state. This interesting and complex field-tuned behavior of the orbital distribution is a consequence of the interplay between the spin-orbit interaction, the octahedral distortions, and the Coulomb repulsion, leading to the possibility of modifying the orbital correlations without a polarization of the ground state. Finally, the field-tuned behavior of the orbital distribution is completely different when one considers the case of an elongated octahedra configuration. Here, for the analyzed microscopic parameters, the OD pattern gets mainly destabilized in favor of AFO configurations.

Further investigation into the direction of correlating the character of the ground state with the transport properties is in progress.

¹For a review, M. Imada, A. Fujimori, and Y. Tokura, *Rev. Mod. Phys.* **70**, 1039 (1998).

²H. F. Pen, J. van den Brink, D. I. Khomskii, and G. A. Sawatzky, *Phys. Rev. Lett.* **78**, 1323 (1997); F. Mila, R. Shiina, F.-C. Zhang, A. Joshi, M. Ma, V. Anisimov, and T. M. Rice, *ibid.* **85**, 1714 (2000).

³G. Khaliullin, P. Horsch, and A. M. Oles, *Phys. Rev. Lett.* **86**, 3879 (2001); P. Horsch, G. Khaliullin, and A. M. Oles, *ibid.* **91**, 257203 (2003).

⁴For a review, *Ruthenate and Rutheno-Cuprate Materials: Unconventional Superconductivity, Magnetism and Quantum Phase Transitions*, edited by C. Noce, A. Vecchione, M. Cuoco, and A. Romano, Springer Lecture Notes in Physics Vol. 603 (Springer-Verlag, Berlin, 2002).

⁵S. Nakatsuji and Y. Maeno, *Phys. Rev. Lett.* **84**, 2666 (2000); *Phys. Rev. B* **62**, 6458 (2000).

⁶T. Mizokawa, L. H. Tjeng, G. A. Sawatzky, G. Ghiringhelli, O. Tjernberg, N. B. Brookes, H. Fukazawa, S. Nakatsuji, and Y. Maeno, *Phys. Rev. Lett.* **87**, 077202 (2001).

⁷I. Zegkinoglou, J. Strempfer, C. S. Nelson, J. P. Hill, J. Chahalian, C. Bernhard, J. C. Lang, G. Srajer, H. Fukazawa, S.

Nakatsuji, Y. Maeno, and B. Keimer, *Phys. Rev. Lett.* **95**, 136401 (2005).

⁸M. Kubota, Y. Murakami, M. Mizumaki, H. Ohsumi, N. Ikeda, S. Nakatsuji, H. Fukazawa, and Y. Maeno, *Phys. Rev. Lett.* **95**, 026401 (2005).

⁹J. S. Lee, Y. S. Lee, T. W. Noh, S.-J. Oh, Jaejun Yu, S. Nakatsuji, H. Fukazawa, and Y. Maeno, *Phys. Rev. Lett.* **89**, 257402 (2002).

¹⁰J. H. Jung, Z. Fang, J. P. He, Y. Kaneko, Y. Okimoto, and Y. Tokura, *Phys. Rev. Lett.* **91**, 056403 (2003).

¹¹G. Cao, L. Balicas, Y. Xin, J. E. Crow, and C. S. Nelson, *Phys. Rev. B* **67**, 184405 (2003).

¹²J. F. Karpus, R. Gupta, H. Barath, S. L. Cooper, and G. Cao, *Phys. Rev. Lett.* **93**, 167205 (2004).

¹³H. L. Liu, S. Yoon, S. L. Cooper, G. Cao, and J. E. Crow, *Phys. Rev. B* **60**, R6980 (1999).

¹⁴G. Cao, L. Balicas, X. N. Lin, S. Chikara, E. Elhami, V. Dairaj, J. W. Brill, R. C. Rai, and J. E. Crow, *Phys. Rev. B* **69**, 014404 (2004).

¹⁵X. N. Lin, Z. X. Zhou, V. Durairaj, P. Schlottmann, and G. Cao, *Phys. Rev. Lett.* **95**, 017203 (2005).

- ¹⁶G. Cao, X. N. Lin, L. Balicas, S. Chikara, J. E. Crow, and P. Schlottmann, *New J. Phys.* **6**, 159 (2004).
- ¹⁷M. Braden, G. André, S. Nakatsuji, and Y. Maeno, *Phys. Rev. B* **58**, 847 (1998).
- ¹⁸S. Nakatsuji and Y. Maeno, *Phys. Rev. B* **62**, 6458 (2000).
- ¹⁹C. S. Snow, S. L. Cooper, G. Cao, J. E. Crow, H. Fukazawa, S. Nakatsuji, and Y. Maeno, *Phys. Rev. Lett.* **89**, 226401 (2002).
- ²⁰F. Nakamura, T. Goko, M. Ito, T. Fujita, S. Nakatsuji, H. Fukazawa, Y. Maeno, P. Alireza, D. Forsythe, and S. R. Julian, *Phys. Rev. B* **65**, 220402(R) (2002).
- ²¹Y. Maeno, H. Hashimoto, K. Yoshida, S. Nishizaki, T. Fujita, J. G. Bednorz, and F. Lichtenberg, *Nature (London)* **372**, 532 (1994); Y. Maeno, T. M. Rice, and M. Sgrist, *Phys. Today* **54**, 42 (2001).
- ²²O. Friedt, M. Braden, G. André, P. Adelman, S. Nakatsuji, and Y. Maeno, *Phys. Rev. B* **63**, 174432 (2001).
- ²³T. Nomura and K. Yamada, *J. Phys. Soc. Jpn.* **69**, 1856 (2000).
- ²⁴S. Okamoto and A. J. Millis, *Phys. Rev. B* **70**, 195120 (2004).
- ²⁵Z. Fang and K. Terakura, *Phys. Rev. B* **64**, 020509(R) (2001); Z. Fang, N. Nagaosa, and K. Terakura, *ibid.* **69**, 045116 (2004).
- ²⁶V. I. Anisimov, I. A. Nekrasov, D. E. Kondakov, T. M. Rice, and M. Sgrist, *Eur. Phys. J. B* **25**, 191 (2002).
- ²⁷A. Koga, N. Kawakami, T. M. Rice, and M. Sgrist, *Phys. Rev. Lett.* **92**, 216402 (2004).
- ²⁸A. Liebsch, *Phys. Rev. B* **70**, 165103 (2004).
- ²⁹S. Biermann, L. de Medici, and A. Georges, *Phys. Rev. Lett.* **95**, 206401 (2005).
- ³⁰T. Hotta and E. Dagotto, *Phys. Rev. Lett.* **88**, 017201 (2002).